

Self-Supervised Learning-Based Cervical Cytology Diagnostics in Low-Data Regime and Low-Resource Setting

Thomas Stegmüller¹, Christian Abbet¹, Behzad Bozorgtabar¹, Holly Clarke², Patrick Petignat², Pierre Vassilakos^{†2}, and Jean-Philippe Thiran^{†1}

¹ EPFL, Lausanne, Switzerland {firstname}.{lastname}@epfl.ch

² HUG, Geneva, Switzerland {Firstname}.{Lastname}@hcuge.ch

Abstract. Screening Papanicolaou test samples effectively reduces cervical cancer-related mortality, but the lack of trained cytopathologists prevents its widespread adoption in low-resource settings. Developing AI algorithms, e.g., deep learning to analyze the digitized cytology images suited to resource-constrained countries is appealing. Albeit successful, it comes at the price of collecting large annotated training datasets, which is both costly and time-consuming. Our study shows that the large number of unlabeled images that can be sampled from digitized cytology slides make for a ripe ground where self-supervised learning methods can thrive and even outperform *off-the-shelf* deep learning models on various downstream tasks. Along the same line, we report improved performance and data efficiency using modern augmentation strategies.

Keywords: Digital cytology · Self-supervised Learning · Low-data Regime.

1 Introduction

Cervical cancer continues to be a major global health concern, with over 600,000 cases diagnosed and over 340,000 deaths reported worldwide in 2020 [27]. The most significant burden of cervical cancer falls on settings that are least equipped to manage the disease, with the vast majority ($\sim 90\%$) of cases affecting low- and middle-income countries (LMIC) [11]. Periodic screening is known to significantly reduce the incidence and mortality of cervical cancer [21]. It is predicted that adequate screening and treatment programs could prevent half of the predicted cervical cancer deaths over the next 50 years [24]. However, effective widespread screening is unobtainable in many countries, partly due to a lack of trained cytopathologists to diagnose Papanicolaou (PAP) tests. Moreover, producing cervical cytological slides is a labor-intensive and sometimes error-prone process [10,26]. Relying exclusively on human papillomavirus (HPV) testing is not a viable alternative diagnostic method due to its poor specificity, which results in overtreatment [17]. The advent of digital microscopy and the recent evidence that digitally based diagnostic performance is on-par with light microscopy for

[†] Joint supervision.

Papanicolaou test slides [16] provides an interesting alternative. The added possibility of incorporating computer-assisted and/or automated diagnostics makes this an even more exciting prospect.

Histopathology-based assessment is considered the “gold standard” for most cancer-related diagnostics, and histology attracts far more attention from the machine learning community [1,25,4] than cytology. Recently though, cytopathology has gained more traction and recognition, as it offers a non-invasive and inexpensive diagnostic tool suited to resource-constrained countries. Consequently, there have been significant advancements in the field of machine learning applied to cytology. Most of these advancements focus on cell-level tasks, e.g., classification [20,2], detection [19,18] or segmentation [14]. These innovations aim to improve the efficiency and accuracy of cervical cancer screening and other forms of cancer diagnosis from cytological samples.

The classification of whole slide Pap smear images remains significantly less studied, despite being most promising in terms of its practical application. Notable works on the topic include [8], which combines low- and high-resolution stages for the identification/localization of suspicious lesions and their classification. The high-resolution stage relies on an RNN-based classification model to predict the WSI-level scores. Another study, [28], leverages a YOLO-based [23] approach to generate cell/tile-level predictions in the first stage, and a transformer model for the aggregation and WSI-level classification in the second stage. Similarly, [5] proposes to integrate an attention module to detect abnormal cells in large patches and compute the abnormality probability of a given patch as the average of its constituent cells. The WSI-level score is obtained by averaging the abnormality of its patches.

Cytology is only starting to attract machine learning practitioners, and, as such, there is relatively little literature on the subject. This work explores the possibilities and challenges of deep learning-based cytology diagnostics and systematically reports our findings. More precisely, we reveal the following facets of pap smear cytology:

- We validate the usage of self-supervised pre-training to learn meaningful representations of cytology images for various downstream tasks. In particular, the resulting representations show superior discriminability and generalizability;
- Representations learned with publicly available single cervical cell datasets, e.g., Herlev [15], or SIPAKMED [22], do not generalize well to different modalities such as images representing multiple cells;
- We experimentally show that we can learn generalizable representations from single-cell datasets with the appropriate data augmentation strategy;
- Multiple instance learning is the *de facto* strategy to obtain WSI-level representations/predictions. Yet, it does not take full advantage of some inherent properties of pap smear cytology slides and is thus sub-optimal. We design a set of simple yet effective modifications to better benefit from the structure of the problem.

2 Datasets

Herlev dataset. A liquid-based cytology Pap smear dataset [15] encompassing 917 labeled cell images. It contains 242 cytology-negative images of annotated cell types of *superficial squamous epithelial* (NS), *intermediate squamous epithelial* (NI), and *Columnar epithelial* (NC). The 675 cytology-positives images are annotated as lesion cells of *mild squamous non-keratinizing dysplasia* (LD), *moderate squamous non-keratinizing dysplasia* (MD), *severe squamous non-keratinizing dysplasia* (SD), and *squamous cell carcinoma in situ intermediate* (CIS), respectively.

Sipakmed dataset. A Pap smear dataset of cervical squamous cells dataset [22] which comprises 4049 labeled cell images. The 1618 cytology-negative images are further categorized as cell types of *superficial-intermediate* (SI) and *parabasal* (P). Similarly, images are annotated as *Koilocytotic* (K) and *dyskeratotic* (D) are represented among the 1638 cytology-positive images. Finally, 793 images representing *metaplastic* (M) cells, which cannot be univocally classified as positives or negatives, are also present in the dataset.

In-house dataset. The performance of our method is assessed on an in-house

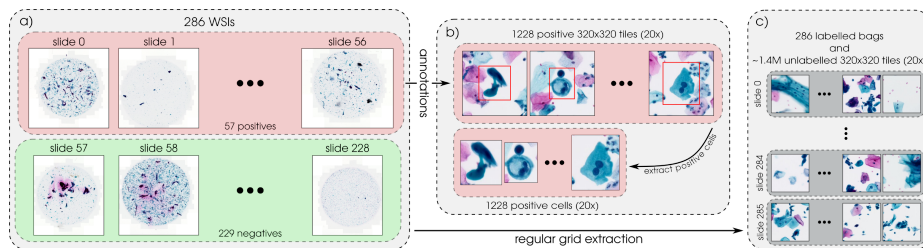


Fig. 1. Overview of the in-house dataset. a) The N WSIs are labelled as positives (N_p samples) or negatives (N_n samples). b) 1228 cell-level annotations are used to extract as many isolated positive cells and 320×320 pixels tiles, both at $20\times$ magnification. c) The tiles of each WSI are extracted based on a regularly spaced grid, yielding $\sim 1.4M$ unlabelled tiles (320×320 pixels and $20\times$ magnification) distributed over 286 slide bags.

cohort of 286 Pap smear slides from HPV-positive patients. The prevalence of cytology-positive slides is approximately 20%, which translates to 57 positive and 229 negative slides. The preparation of the slides follows the SurePathTM procedure. This choice is motivated by the overall objective: remote diagnosis of cervical smears for the triage of HPV-positive women in a resource-limited setting. Indeed, this preparation yields a small cell-deposit area, which shortens the scanning time and reduces the size of the digitized slides. Additionally, the SurePathTM procedure exists in a manual and low-cost version to further ease its adoption in a low-income setting. Along the same line, the slides are digitized with the Grundium Ocus[®]40 scanner: a portable and affordable solution. The

WSIs are acquired with a 12 megapixels image sensor, a 40x objective, and Z-stacking (3 focal planes spaced by $1\mu m$).

After digitization, cell-level annotations are obtained using QuPath[3], resulting in 1228 annotated positive cells. The annotations are used to create a dataset of 1228 positive cell images and as many positive 320×320 pixels tiles (cell+context, see Fig. 1) both at $20\times$ magnification ($0.50 \mu m/px$). Alternatively, we create an unlabeled tile dataset by finding the cell-deposit area with standard image processing techniques and subsequently sampling 320×320 tiles on a regular grid without overlap, yielding approximately 1.5M images, subdivided into 307 bags encompassing an average of 5200 tiles each. The bags are used for WSI-level classification, whereas the individual tiles serve as a substrate for the SSL pre-training (see Sec. 3.1). We use a stratified 4-fold split approach to partition the slides into training, validation, and test subsets. The slide-level splits are common to all experiments, including the SSL pre-training.

3 Deep Cytology Under Scrutiny

In Section 1, we evoke the urge to develop robust methods for diagnosing cervical cancer based on Pap smear cytology in a low-resource setting. The emergence of affordable and transportable high-resolution scanners, e.g., **Grundium Ocus[®]40**, as well as the existence of low-cost slides preparation procedures (SurePath[™]) make for a particularly ripe ground for this enterprise. Regarding the learning algorithm, most costs can be attributed to the annotation procedure and the level of expertise it requires. As such, we thoroughly investigate the usage of non-label intensive methods for cytology-related tasks and report our findings.

3.1 Can cytology benefit from self-supervised pre-training?

Compared to histology, cytology has received little attention, and there is little evidence of the feasibility of using SSL methods on Pap-smear cytology images. Indeed, most state-of-the-art SSL methods [12,29,6,7] for image-level representations learning rely on maximizing the similarity of an image’s representation under information preserving transformations. Crucially, one of these transformations is a spatial crop, which is at risk of losing its information-preserving property on cytology images due to the preparation of the slides that break long-range spatial dependencies. Nonetheless, each slide can yield thousands of unlabelled images, which hints that cytology could enormously benefit from a self-supervised pre-training.

The SSL framework used to pre-train our models is DINO [7]. We experiment with two standard architectures, ResNet50 [13], and ViT-S/16 [9], for which we use the recommended parameters available on the official **repository**. The arguments only differ from the recommendations for the batch size and the number of local crops. The batch size is set to fill the available GPU memory, i.e., `batch_size = 256` for a ResNet50 and `batch_size = 192` for a ViT-S/16. We do not use local crops as they can result in ambiguous positive pairs for

non-object-centric datasets, as is the case here. For each architecture, we train one model per stratified split ($\sim 1\text{M}$ tiles of 320×320 pixels at a magnification of $20\times$) for 300 epochs.

Cell-level classification. We probe the quality of the learned features on a cell-level classification task (see Tables 1 & 2). We use two publicly available cervical cell Pap smear datasets: Herlev [15], and Sipakmed [22]. The datasets are randomly split in train/validation with a 75/25 partition, and we report the mean and standard deviation of the class-wise and weighted F_1 score over 4 independent runs. The number of neighbors k is the one that maximizes the weighted F_1 score.

Table 1. Cell-level classification on the Herlev dataset. We report the class-wise and weighted F_1 score of a k -NN classifier. The features are extracted by a ViT-S/16 or a ResNet50 pre-trained under a supervised pre-training on ImageNet or a self-supervised pre-training on our internal dataset with DINO [7].

<i>positives</i>				<i>negatives</i>			<i>average</i>		
CIS	LD	MD	SD	NC	NI	NS	positives	negatives	weighted F1
<i>ResNet50</i>									
55.0 \pm 4.5	64.3 \pm 5.3	48.6 \pm 4.8	51.3 \pm 3.7	53.8 \pm 4.1	87.0 \pm 7.5	89.6 \pm 6.3	93.2 \pm 0.6	80.1 \pm 1.7	60.2 \pm 3.2
59.0 \pm 7.1	66.2 \pm 3.7	48.6 \pm 6.8	53.0 \pm 4.9	50.9 \pm 8.0	88.8 \pm 5.2	92.4 \pm 2.8	92.3 \pm 1.5	78.6 \pm 3.8	61.7 \pm 3.2
<i>ViT-S/16</i>									
55.1 \pm 5.7	59.5 \pm 3.2	38.6 \pm 8.2	48.7 \pm 3.1	49.2 \pm 4.6	75.8 \pm 5.1	83.2 \pm 7.2	92.4 \pm 1.1	76.8 \pm 2.4	55.2 \pm 2.0
62.8 \pm 4.4	66.8 \pm 4.5	48.2 \pm 5.1	53.5 \pm 5.5	58.8 \pm 7.5	83.4 \pm 1.9	89.7 \pm 3.2	93.1 \pm 0.9	80.8 \pm 2.9	62.6 \pm 2.8

Table 2. Cell-level classification on the Sipakmed dataset. We report the class-wise and weighted F_1 score of a k -NN classifier. The features are extracted by a ViT-S/16 or a ResNet50 pre-trained under a supervised pre-training on ImageNet or a self-supervised pre-training on our internal dataset with DINO [7].

<i>positives</i>		-	<i>negatives</i>		<i>average</i>		
D	K	M	P	SI	positives	negatives	weighted F1
<i>ResNet50</i>							
94.4 \pm 1.1	85.6 \pm 1.2	90.4 \pm 0.6	95.9 \pm 0.5	97.0 \pm 0.7	95.9 \pm 0.2	96.1 \pm 0.2	92.6 \pm 0.4
93.5 \pm 1.2	87.7 \pm 1.7	91.6 \pm 1.1	97.2 \pm 0.9	98.7 \pm 0.6	97.2 \pm 0.5	97.3 \pm 0.5	93.7 \pm 0.7
<i>ViT-S/16</i>							
91.2 \pm 0.8	82.1 \pm 1.4	86.3 \pm 0.7	94.9 \pm 0.6	94.0 \pm 0.8	95.1 \pm 0.8	95.4 \pm 0.7	89.7 \pm 0.5
94.9 \pm 0.7	88.8 \pm 0.8	91.8 \pm 0.9	98.0 \pm 0.6	98.7 \pm 0.7	97.6 \pm 0.4	97.6 \pm 0.3	94.4 \pm 0.3

Cell-level transfer learning. Here, we examine the generalizability of the learned features. The embeddings of the samples from the Herlev and Sipakmed datasets are used as support sets to fit a k -NN classifier, which is subsequently evaluated on the internal cell dataset (see Table 3). The whole source and target

datasets are used; hence the randomness in the results is due to the multiplicity of the DINO pre-trained models. The number of neighbors k is the one that maximizes the weighted F_1 score.

Table 3. Transfer learning from the Herlev [15] and/or Sipakmed dataset [22] to our in-house cells and tiles dataset. A k -NN classifier is fitted on the binary version of Herlev (H) and/or Sipakmed (S) datasets and evaluated on the in-house set of positive cells/tiles; hence the sensitivity is reported. The features are extracted by a ViT-S/16 or a ResNet50 pre-trained under a supervised pre-training on ImageNet or a self-supervised pre-training on our internal dataset with DINO [7].

<i>model</i>	<i>cells → cells</i>			<i>cells → tiles</i>		
	H	S	H+S	H	S	H+S
ResNet50	93.7	67.4	68.1	62.0	16.3	17.1
ResNet50	68.6 ± 5.8	84.0 ± 4.0	82.1 ± 3.8	57.9 ± 6.4	25.1 ± 6.6	31.7 ± 4.9
ViT-S/16	92.5	56.7	57.4	80.7	22.1	21.2
ViT-S/16	82.9 ± 1.7	80.7 ± 1.3	79.7 ± 1.7	69.5 ± 4.3	63.6 ± 2.1	63.5 ± 2.4

4 Conclusion

Reliable automation of cytology diagnostics is still a long way ahead of us, and progress in the field is hindered by the small amount of publicly labeled datasets. Our work reveals that self-supervised learning and strong data augmentation strategies can be leveraged to make the most out of the available data and even surpass *off-the-shelf* supervised deep learning models. Future work will extend the discussed methods to more challenging tasks, such as positive cell detection and segmentation.

References

1. Abbet, C., Studer, L., Fischer, A., Dawson, H., Zlobec, I., Bozorgtabar, B., Thiran, J.P.: Self-rule to multi-adapt: Generalized multi-source feature learning using unsupervised domain adaptation for colorectal cancer tissue detection. *Medical Image Analysis* **79**, 102473 (2022). <https://doi.org/https://doi.org/10.1016/j.media.2022.102473>, <https://www.sciencedirect.com/science/article/pii/S1361841522001207> **2**
2. Albuquerque, T., Cruz, R., Cardoso, J.S.: Ordinal losses for classification of cervical cancer risk. *PeerJ Computer Science* **7**, e457 (2021) **2**
3. Bankhead, P., Loughrey, M.B., Fernández, J.A., Dombrowski, Y., McArt, D.G., Dunne, P.D., McQuaid, S., Gray, R.T., Murray, L.J., Coleman, H.G., et al.: Qupath: Open source software for digital pathology image analysis. *Scientific reports* **7**(1), 1–7 (2017) **4**
4. Bozorgtabar, B., Vray, G., Mahapatra, D., Thiran, J.P.: Sood: Self-supervised out-of-distribution detection under domain shift for multi-class colorectal cancer tissue types. In: *Proceedings of the IEEE/CVF International Conference on Computer Vision*. pp. 3324–3333 (2021) **2**
5. Cao, L., Yang, J., Rong, Z., Li, L., Xia, B., You, C., Lou, G., Jiang, L., Du, C., Meng, H., et al.: A novel attention-guided convolutional network for the detection of abnormal cervical cells in cervical cancer screening. *Medical image analysis* **73**, 102197 (2021) **2**
6. Caron, M., Misra, I., Mairal, J., Goyal, P., Bojanowski, P., Joulin, A.: Unsupervised learning of visual features by contrasting cluster assignments. In: *Thirty-fourth Conference on Neural Information Processing Systems (NeurIPS)* (2020) **4**
7. Caron, M., Touvron, H., Misra, I., Jégou, H., Mairal, J., Bojanowski, P., Joulin, A.: Emerging properties in self-supervised vision transformers. *arXiv preprint arXiv:2104.14294* (2021) **4, 5, 6**
8. Cheng, S., Liu, S., Yu, J., Rao, G., Xiao, Y., Han, W., Zhu, W., Lv, X., Li, N., Cai, J., et al.: Robust whole slide image analysis for cervical cancer screening using deep learning. *Nature communications* **12**(1), 1–10 (2021) **2**
9. Dosovitskiy, A., Beyer, L., Kolesnikov, A., Weissenborn, D., Zhai, X., Unterthiner, T., Dehghani, M., Minderer, M., Heigold, G., Gelly, S., et al.: An image is worth 16x16 words: Transformers for image recognition at scale. *arXiv preprint arXiv:2010.11929* (2020) **4**
10. Elsheikh, T.M., Austin, R.M., Chhieng, D.F., Miller, F.S., Moriarty, A.T., Renshaw, A.A.: American society of cytopathology workload recommendations for automated pap test screening: Developed by the productivity and quality assurance in the era of automated screening task force. *Diagnostic cytopathology* **41**(2), 174–178 (2013) **1**
11. Gultekin, M., Ramirez, P.T., Broutet, N., Hutubessy, R.: World health organization call for action to eliminate cervical cancer globally. *International Journal of Gynecological Cancer* **30**(4), 426–427 (2020) **1**
12. He, K., Fan, H., Wu, Y., Xie, S., Girshick, R.: Momentum contrast for unsupervised visual representation learning. In: *Proceedings of the IEEE/CVF Conference on Computer Vision and Pattern Recognition*. pp. 9729–9738 (2020) **4**
13. He, K., Zhang, X., Ren, S., Sun, J.: Deep residual learning for image recognition. In: *Proceedings of the IEEE conference on computer vision and pattern recognition*. pp. 770–778 (2016) **4**

14. Hussain, E., Mahanta, L.B., Das, C.R., Choudhury, M., Chowdhury, M.: A shape context fully convolutional neural network for segmentation and classification of cervical nuclei in pap smear images. *Artificial Intelligence in Medicine* **107**, 101897 (2020) [2](#)
15. Jantzen, J., Norup, J., Dounias, G., Bjerregaard, B.: Pap-smear benchmark data for pattern classification. *Nature inspired Smart Information Systems (NiSIS 2005)* pp. 1–9 (2005) [2](#), [3](#), [5](#), [6](#)
16. Kholová, I., Negri, G., Nasioutziki, M., Ventura, L., Capitanio, A., Bongiovanni, M., Cross, P.A., Bourgain, C., Edvardsson, H., Granados, R., et al.: Inter-and intraobserver agreement in whole-slide digital thinprep samples of low-grade squamous lesions of the cervix uteri with known high-risk hpv status: A multicentric international study. *Cancer Cytopathology* **130**(12), 939–948 (2022) [2](#)
17. Kuhn, L., Saidu, R., Boa, R., Tergas, A., Moodley, J., Persing, D., Campbell, S., Tsai, W.Y., Wright, T.C., Denny, L.: Clinical evaluation of modifications to a human papillomavirus assay to optimise its utility for cervical cancer screening in low-resource settings: a diagnostic accuracy study. *The Lancet Global Health* **8**(2), e296–e304 (2020) [1](#)
18. Li, X., Li, Q., et al.: Detection and classification of cervical exfoliated cells based on faster r-cnn. In: 2019 IEEE 11th international conference on advanced infocomm technology (ICAIT). pp. 52–57. IEEE (2019) [2](#)
19. Liang, Y., Pan, C., Sun, W., Liu, Q., Du, Y.: Global context-aware cervical cell detection with soft scale anchor matching. *Computer Methods and Programs in Biomedicine* **204**, 106061 (2021) [2](#)
20. Lin, H., Hu, Y., Chen, S., Yao, J., Zhang, L.: Fine-grained classification of cervical cells using morphological and appearance based convolutional neural networks. *IEEE Access* **7**, 71541–71549 (2019) [2](#)
21. Peto, J., Gilham, C., Fletcher, O., Matthews, F.E.: The cervical cancer epidemic that screening has prevented in the uk. *The Lancet* **364**(9430), 249–256 (2004) [1](#)
22. Plissiti, M.E., Dimitrakopoulos, P., Sfikas, G., Nikou, C., Krikoni, O., Charchanti, A.: Sipakmed: A new dataset for feature and image based classification of normal and pathological cervical cells in pap smear images. In: 2018 25th IEEE International Conference on Image Processing (ICIP). pp. 3144–3148 (2018). <https://doi.org/10.1109/ICIP.2018.8451588> [2](#), [3](#), [5](#), [6](#)
23. Redmon, J., Farhadi, A.: Yolov3: An incremental improvement. arXiv preprint arXiv:1804.02767 (2018) [2](#)
24. Simms, K.T., Steinberg, J., Caruana, M., Smith, M.A., Lew, J.B., Soerjomataram, I., Castle, P.E., Bray, F., Canfell, K.: Impact of scaled up human papillomavirus vaccination and cervical screening and the potential for global elimination of cervical cancer in 181 countries, 2020–99: a modelling study. *The lancet oncology* **20**(3), 394–407 (2019) [1](#)
25. Stegmüller, T., Bozorgtabar, B., Spahr, A., Thiran, J.P.: Scorenet: Learning non-uniform attention and augmentation for transformer-based histopathological image classification. In: Proceedings of the IEEE/CVF Winter Conference on Applications of Computer Vision. pp. 6170–6179 (2023) [2](#)
26. Stoler, M.H., Schiffman, M., et al.: Interobserver reproducibility of cervical cytologic and histologic interpretations: realistic estimates from the ascus-lsil triage study. *Jama* **285**(11), 1500–1505 (2001) [1](#)
27. Sung, H., Ferlay, J., Siegel, R.L., Laversanne, M., Soerjomataram, I., Jemal, A., Bray, F.: Global cancer statistics 2020: Globocan estimates of incidence and mortality worldwide for 36 cancers in 185 countries. *CA: a cancer journal for clinicians* **71**(3), 209–249 (2021) [1](#)

28. Wei, Z., Cheng, S., Liu, X., Zeng, S.: An efficient cervical whole slide image analysis framework based on multi-scale semantic and spatial deep features. arXiv preprint arXiv:2106.15113 (2021) [2](#)
29. Zhou, J., Wei, C., Wang, H., Shen, W., Xie, C., Yuille, A., Kong, T.: ibot: Image bert pre-training with online tokenizer. arXiv preprint arXiv:2111.07832 (2021) [4](#)